

Quantitative Proteomic Analysis of Dystrophic Dog Muscle

Laetitia Guevel,^{*,†} Jessie R. Lavoie,^{‡,#} Carolina Perez-Iratxeta,^{‡,#} Karl Rouger,^{||} Laurence Dubreil,^{||} Marie Feron,[†] Sophie Talon,[†] Marjorie Brand,^{‡,§,#} and Lynn A. Megeney^{‡,§,#}

[†]CNRS UMR6204, Faculté des Sciences et des Techniques, F-44322 Nantes Cedex 3, France

[‡]Sprott Center for Stem Cell Research, Ottawa Hospital Research Institute, Ottawa, ON Canada K1H 8L6

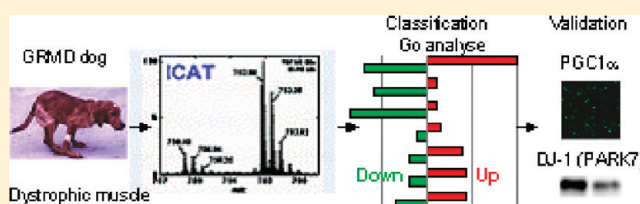
[§]Department of Medicine and Cellular and Molecular Medicine, University of Ottawa, Ottawa, ON K1H 8M5

^{||}INRA UMR703, Ecole Nationale Vétérinaire, Oniris, F-44307 Nantes Cedex 3, France

S Supporting Information

ABSTRACT: Duchenne muscular dystrophy (DMD) is caused by null mutations in the dystrophin gene, leading to progressive and unrelenting muscle loss. Although the genetic basis of DMD is well resolved, the cellular mechanisms associated with the physiopathology remain largely unknown. Increasing evidence suggests that secondary mechanisms, as the alteration of key signaling pathways, may play an important role. In order to identify reliable biomarkers and potential therapeutic targets, and taking advantage of the clinically relevant Golden Retriever Muscular Dystrophy (GRMD) dog model, a proteomic study was performed. Isotope-coded affinity tag (ICAT) profiling was used to compile quantitative changes in protein expression profiles of the *vastus lateralis* muscles of 4-month old GRMD vs healthy dogs. Interestingly, the set of under-expressed proteins detected appeared primarily composed of metabolic proteins, many of which have been shown to be regulated by the transcriptional peroxisome proliferator-activated receptor- γ co-activator 1 α (PGC-1 α). Subsequently, we were able to show that PGC-1 α expression is dramatically reduced in GRMD compared to healthy muscle. Collectively, these results provide novel insights into the molecular pathology of the clinically relevant animal model of DMD, and indicate that defective energy metabolism is a central hallmark of the disease in the canine model.

KEYWORDS: Duchenne muscular dystrophy, GRMD dog, PGC-1 α , quantitative proteomic, ICAT/MS/MS



INTRODUCTION

Duchenne muscular dystrophy (DMD) is a recessive X-linked neuromuscular disorder affecting one newborn boy in 3500.¹ DMD is caused by mutations in the dystrophin gene,^{2–4} and is characterized by severe degeneration of muscle fibers, progressive paralysis, and ultimately, death. The dystrophin protein is localized under the sarcolemma of muscle fibers and is integrated within a large multiprotein complex (the dystrophin–glycoprotein complex, DGC), which provides a strong physical link between the actin cytoskeleton network and the extracellular matrix.^{5–8} The absence of dystrophin in dystrophic muscles, which is associated with the subsequent loss of the DGC at the sarcolemma, leads to altered myofiber integrity, perturbed calcium homeostasis, activation of the calcium-dependent calpain proteases, and necrosis.^{9,10}

In addition to the increased structural fragility of DMD myofibers, accumulating evidence suggests that nonmechanical processes also contribute to pathology progression. First, the DGC is associated with several signaling molecules.^{11–13} Second, studies performed in the *mdx* mouse, the murine model of DMD,¹⁴ revealed changes in the MAPK and PI3K/Akt signaling cascades in dystrophic muscles.^{15–18} More recently, the phosphorylation status of Akt was also shown to be altered in human dystrophic biopsies,¹⁷ and we revealed that the PTEN phosphatase

was differentially activated in dystrophic dog muscle, leading to the deregulation of the PI3K/Akt signaling pathway.¹⁹ Collectively, these studies suggest that alterations in signal transduction pathways are significant contributing factors to the progression of DMD. Importantly, some recent studies have also suggested that the modulation of signaling molecules could affect the disease outcome.^{20,21}

However, despite the compelling evidence demonstrating the alteration of individual signaling proteins in dystrophic muscle, little is known regarding the involvement of the corresponding signaling pathways in the development of the disease. In addition, only limited knowledge is available regarding the impact of dystrophin loss on the muscle proteome. Interestingly, proteomic profiling studies of the *mdx* mouse model revealed that the expression level of numerous proteins involved in the maintenance of sarcolemmal integrity (i.e., Fbxo11, adenylate kinase, the Ca²⁺ binding protein regucalin, and cvHSP) was altered in dystrophin–deficient fibers.^{22–24} One of the most interesting aspects of the *mdx* mouse is that it contains subtypes of skeletal muscle that exhibit very different degrees of fiber wasting despite the fact that they all contain the same disease-associated mutation in

Received: December 16, 2010

Published: March 16, 2011

exon 23.²⁵ In mature limb muscle, the murine model is characterized by successive degeneration/regeneration processes and does not exhibit the progressive muscle wasting and accumulation of connective tissue observed during development of the human disease.^{26–28} However, aged *mdx* muscles and the *mdx* diaphragm show a severe dystrophic phenotype and histological alterations closely resembling those of the DMD phenotype.^{25,29–31} Another animal model of DMD, the canine Golden Retriever Muscular Dystrophy (GRMD), reflects both the genotype and phenotype of DMD. Affected dogs represents an accurate clinical phenocopy of DMD patients, as they are characterized by rapid progressive clinical dysfunction, severe muscle weakness, and abundant fiber necrosis.^{32,33}

We have recently shown that the perturbations detected within the PI3K/Akt and MAPK signaling pathways in dystrophic dog muscle could differ from the observations made in the *mdx* mouse model, which supports the importance of studying cell signaling events and secondary changes in the clinically relevant animal model.¹⁹ Since there is an urgent need for the establishment of reliable biomarkers of secondary changes in muscular dystrophy, the proteomic study on GRMD muscle is crucial to completed previous proteomic profiling from the dystrophin-deficient *mdx* mouse. We studied the proteome variations between *vastus lateralis* muscle of 4-month old GRMD and healthy dogs. At this stage, skeletal muscles are severely dystrophic and are characterized by high fiber-size variation, individual necrotic fibers, centrally nucleated fibers and fibrosis.^{32,33} We used isotope-coded affinity tag (ICAT) labeling followed by LC–MS/MS to analyzed the quantitative variations of the proteome in both a cytoplasmic fraction and a phospho-enriched fraction prepared from total extracts.³⁴ We chose to analyze the phospho-enriched fraction since protein phosphorylation plays a key role in regulating most cellular processes including proliferation, migration, apoptosis, and metabolic pathways. ICAT experiments revealed a significant alteration of the abundance of 85 proteins. Functional annotation of these proteins indicated a dysregulation in glycolytic and oxidative metabolism. In addition, we discovered that a significant number of proteins expressed at lower levels in the dystrophic samples are coded by genes whose expression is responsive to the peroxisome proliferator-activated receptor-gamma co-activator 1 alpha (PGC- α) a master switch for the transcriptional control of energy metabolism.³⁵ Accordingly, we showed that PGC-1 α level is substantially reduced in GRMD muscle. Taken together, our results provide compelling new evidence that defects in energy metabolism are a hallmark of the disease in the canine model, and that in turn, these defects may contribute to the disease progression.

EXPERIMENTAL PROCEDURES

Products

Ammonium bicarbonate (NH₄HCO₃), dibasic sodium phosphate (Na₂HPO₄), monobasic sodium phosphate (NaH₂PO₄), sodium chloride (NaCl), Tris, Triton X-100, and bicinchoninic acid (BCA) protein assay reagents were purchased from Sigma-Aldrich (St. Louis, MO). Trifluoroacetic acid and formic acid were obtained from Fluka (Milwaukee, WI). High-performance liquid chromatography grade acetonitrile (ACN: CH₃CN) and methanol (CH₃OH) were obtained from Fisher Scientific (Fair Lawn, NJ). Cleavable ICAT reagents, monomeric avidin, and SCX cartridges were purchased from Applied Biosystems, Inc. (Foster City, CA).

Animals

Animals were part of a GRMD dog breeding colony established in Nantes (France). They were housed and cared for at the

Boisbonne Center for Gene Therapy of the National Veterinary School of Nantes, following protocols compliant with the principles outlined in the French National Institute for Agronomic Research (INRA) Guide for the care and use of laboratory animals in biological experimentation. Affected dogs were identified during the first days of life by polymerase chain reaction genotyping using appropriate oligonucleotide primers and immunohistochemical localization of dystrophin. Four-month old GRMD dogs from Nantes colony are less active than normal littermates. They are defined by a decreased mobility and appear tired during minimal exercise.^{32,36} Their body weight is lower than that of unaffected littermates. While normal littermates display coordinated gait, GRMD dogs are characterized by an abnormal, stiff-limbed, shuffling gait and a marked weight transfer. Another prominent sign characteristic of muscular dystrophy is palmigrade/plantigrade stances.

Muscles

GRMD and healthy littermates (GRMD dog#1, #2, #3; healthy dog#1, #2, #3) from 4-month old dogs were sacrificed by intravenous sodium pentobarbital administration after general anesthesia and small 1 cm³ pieces of *vastus lateralis* muscle were cut and immediately frozen in liquid nitrogen during 2 min. Then, tissues were stored at –80 °C until processing. For protein extraction, the adipose portions of biopsies were carefully removed manually under a binocular microscope. Muscles were then powdered in liquid nitrogen, and homogenized in modified RIPA lysis buffer containing 150 mM NaCl, 50 mM Tris-HCl, pH 7.4, 1% (v/v) Nonidet-P40, 1% (v/v) glycerol, 1 mM EDTA, protease inhibitors cocktail (Sigma-Aldrich), and 10 mM of the tyrosine phosphatase inhibitor sodium orthovanadate. Homogenates were centrifuged at 1000g to pellet debris, and supernatants were centrifuged at 37 000g for 20 min at 4 °C to fractionate cytosolic proteins. Protein concentration was determined using a BCA protein assay. For ICAT/MS/MS analysis, a total of 80 μ g of cytosolic proteins (GRMD dog#1; healthy dog#1) was subjected to buffer-exchange in TE pH 8.3 containing 50 mM NaCl. For the histopathological analysis, the sectioned blocks were embedded in Tissue-Tek O.C.T. compound (Sakura Finetek, Torrance, CA), and frozen in isopentane cooled with liquid nitrogen. Transverse *vastus lateralis* muscle cryosections (8 μ m) were prepared using a Leica CM 3050S cryostat. Hematoxylin & eosin (H&E) was performed as per standard histological protocols.³⁷

Phosphoprotein Enrichment

Phosphoprotein enriched fractions were prepared from healthy and dystrophic muscles (GRMD dog#2; healthy dog#2) using a commercially available PhosphoProtein Purification Kit (Qiagen; Missisauga, CA).³⁸ The eluate was precipitated with TCA/acetone and the pellet was dissolved in ICAT labeling buffer (0.05% (w/v) SDS, 20 mM Tris-HCl, pH 8.3, 5 mM EDTA, 6 M urea). Protein concentration was measured using a BCA assay and a total of 30 μ g of proteins was used for the ICAT/MS/MS analysis.

cICAT Labeling and Mass Spectrometry

Healthy and dystrophic cytosolic and phospho-enriched proteins (80 and 30 μ g, respectively, $n = 1$ for each fraction) were labeled with the acid-cleavable ICAT reagent (cICAT) (Applied Biosystems, Framingham, MA) and analyzed by mass spectrometry as previously described,³⁹ with the following modifications. Proteins from the healthy and dystrophic muscle were

labeled with the isotopically light form of cICAT [$^{12}\text{C}_9$] and the isotopically heavy form of cICAT [$^{13}\text{C}_9$], respectively. Labeled proteins were combined and proteolyzed with trypsin (Promega, Madison, WI). Resulting peptides were separated into 4 fractions by cation-exchange chromatography, and cICAT-labeled peptides were purified from each fraction by avidin-affinity chromatography.³⁹ Labeled peptides from the 4 fractions were analyzed by microcapillary reverse phase liquid chromatography electrospray ionization, followed by tandem mass spectrometry ($\mu\text{LC-ESI-MS/MS}$) using an ion trap mass spectrometer (LTQ, Thermofinnigan). Briefly, peptides were dried under vacuum, dissolved in a buffer containing 10% (v/v) ACN and 0.1% (v/v) trifluoroacetic acid (TFA), and pressure loaded onto an in-house prepared 10-cm \times 75 μm fused silica microcapillary column packed with 5 μm Magic C18 beads. Peptides were resolved using an 80 min separation gradient from 2 to 50% HPLC Buffer (100% (v/v) ACN, 0.1% (v/v) HCOOH) at a 300 nL/min flow rate. The mass spectrometer was set to scan from 400 to 1800 m/z followed by two data-dependent MS/MS scans on the two most abundant ions. Dynamic exclusion was set to exclude ions that have been selected for MS/MS analysis for 2 min with a mass window of 2 Da.

ICAT Data Analysis

Raw data was converted to mzXML using ReAdW. MS/MS spectra were then exported as data files and searched against the ENSEMBL49 dog database, which contains 25 559 protein entries. The search was performed using SEQUEST (v 3.3.1 SP1), a data analysis program used for protein identification.⁴⁰ The mass of cysteine was statically modified by 227.13 Da (light cICAT) and differentially modified by 9.03 Da (heavy cICAT). Methionine was differentially modified as well with 16 Da to account for its oxidized form. Peptides identified by SEQUEST were analyzed using the Trans Proteomics Pipeline (TPP) (version 3.4) mirroring the TPP at the Seattle Proteome Center. This pipeline uses the PeptideProphet⁴¹ and ProteinProphet⁴² algorithms to, respectively, validate the peptide and protein assignments to the MS/MS spectra made by SEQUEST, and to compute the probability that the assignments are correct. For the peptides database searches, we used a probability cutoff of 0.9 that corresponds to an overall false positive error rate below 0.6% for the cytoplasmic proteins, and 0.8% for the phospho-enriched proteins.⁴³

Relative quantification of proteins (Light-labeled vs Heavy-labeled) was performed within the TPP using the ASAP ratio program,⁴⁴ an algorithm evaluating protein abundance ratios (i.e., ICAT ratios). For quantification of cytoplasmic proteins, 90% of the proteins with 2 or more quantified peptide ions have a relative error smaller than 22%. For quantification of phospho-enriched proteins, 62% of the proteins with 2 or more quantified peptide ions have a relative error smaller than 22%. The quality of each spectrum used for identification and quantification was verified manually. A value of ± 0.5 for the log₂ transformed and centered ASAP ratios was chosen as the cutoff threshold for significantly over/under represented proteins. We considered the proteins with a relative level between healthy and dystrophic muscles comprised outside the interval [0.7-fold; 1.42-fold] as significantly over/under represented.

Immunoblot Assays

To validate the protein changes detected by proteomic analyses, immunoblotting experiments were performed on a representative range of protein types. Cytosolic protein extracts

(GRMD dog#1, #2, #3; healthy dog#1, #2, #3) were resolved by sodium dodecyl sulfate–polyacrylamide gel electrophoresis (SDS–PAGE) on 10% polyacrylamide gels and electroblotted onto immobilon-P membranes (Millipore Corp., Bedford, MA). Blots were blocked with PBS containing 0.1% (v/v) Tween-20, 2.5% (w/v) BSA at room temperature for 1 h, and then incubated with sufficiently diluted primary antibodies against DJ-1, protein phosphatase 1 (PP1), alpha tubulin, lactate dehydrogenase (LDHA), cofilin 2, and pyruvate kinase type M2 (PKM2). Anti-DJ-1, anti-PP1, anti-LDHA, and anti-PKM2 were obtained from Cell Signaling Technology (Beverly, MA). Anti-cofilin 2 was obtained from Abcam (Cambridge, MA). The incubation was performed for 2 h at room temperature in PBS containing 0.1% Tween-20 and 1% BSA. Immunoreactivity was visualized by peroxidase-conjugated secondary antibodies and by SuperSignal West Pico chemiluminescence substrate (Pierce, Rockford, IL). Equal protein loading was verified through a Ponceau red staining of the membranes. The Western blot analyses were conducted using biopsies removed from three different dogs and the average value was calculated.

PGC-1 α Immunohistological Analysis

To determine the location of PGC-1 α , a double labeling directed against PGC-1 α and β -dystroglycan (β -DG), which is expressed in the plasma membrane of healthy muscles (while it is highly reduced in the dystrophic ones⁴⁵) was performed, in association with nuclei staining. Transverse *vastus lateralis* muscle cryosections (GRMD dog#1, #2, #3; healthy dog#1, #2) (8 μm) were prepared using a Leica CM 3050S cryostat. Sections were fixed with methanol and acetone at -20°C and permeabilized by an incubation in PBS containing 0.3% TX-100 at room temperature for 5 min. They were then blocked with 10% goat serum in PBS containing 0.3% TX-100 for 30 min, and finally incubated in blocking solution at 4°C with a rabbit polyclonal antibody against PGC-1 α (1:50; Santa Cruz Biotechnology, Santa Cruz, CA). After washing with PBS, the sections were incubated 1 h at room temperature with a goat anti-rabbit secondary antibody labeled with Alexa fluor 488 (1:400; Invitrogen Life Technologies, CA). After washing, the samples were incubated for 1 h at 37°C with a mouse monoclonal antibody against β -dystroglycan (1/50, Novocastra), a plasma membrane component. Sections were then washed and incubated for 1 h at room temperature with an Alexa fluor 555 goat anti-mouse antibody (1/400, Invitrogen Life Technologies, CA). Nuclei were stained with Topro-3 (1/1000, Invitrogen Life Technologies). Slides were finally coverslipped and mounted with Mowiol Medium (Calbiochem EMD Biosciences, San Diego, CA). The immunolabeled sections were serially scanned with a confocal microscope (Nikon C1, Champigny-sur-Marne, France) using the argon ion laser (488 nm) to observe PGC-1 α immunolabeling, a 543 nm helium neon laser to observe β -dystroglycan immunolabeling, and a 633 nm helium neon laser to observe nuclei stained.

Real-Time Reverse Transcription PCR

The genes coding for the PGC-1 α protein (PPARGC1 α) and its putative altered downstream targets (ACADS, FABP3, CYC1 and PFKM), chosen in the list presented in Figure 3A were analyzed by real-time RT-PCR. The LDHA gene was used as an internal reference gene, owing to its poor variation (based on our proteomic and transcriptional analysis) among different replicates and conditions. Primers were generated by the oligo 4.0 S software (National Biosciences, Plymouth, MN) and then submitted to BLASTn analysis (NCBI) to confirm their specificity.

All primers were synthesized by Eurofins MWG GmbH (Germany) with the following sequences: for PPARGC1alpha, forward, 5'-ATGTGCTGCTCTGGTTGGTG-3'; reverse, 5'-AGCAAGTTCGCCTCGTTCTC-3'; for ACADS, forward, 5'-TGAACCAGGGAACGGCAG-3'; reverse, 5'-CTTCCTTCTTCCCAGCGT-3'; for FABP3, forward, 5'-ATCAGCTTCAAGTTAGGGGTGG-3'; reverse, 5'-CCATCAACTAGCTCCCAGCA-3'; for CYC1, forward, 5'-AGTGATGCTGTCGGCGTTG-3'; reverse, 5'-CCGTCTGAACCTCCACCT-3'; for PFKM, forward, 5'-GTGGGGCTGACTGGGTTTT-3'; reverse, 5'-ATCACTGCTTCCACACCCATC-3'; for LDHA, forward, 5'-GCTGGTTATTATCACGGC-3'; reverse, 5'-TCCCAACCTTTCCCCCA-3'.

Total RNA extraction was performed from muscular biopsies of GRMD and healthy dogs (GRMD dog#1, #2, #3; healthy dog#2, #3) by using the RNeasy Fibrous Tissue Mini Kit (Qiagen) according to manufacturer's instructions. For the real-time PCR, 0.5 μ g of total RNA was first reverse-transcribed using the Superscript II reverse transcriptase (Invitrogen) according to the manufacturer's recommendations. Then, cDNA targets were amplified in triplicate wells using the MESABlue qPCR MasterMix Plus for SYBR Assay w/fluorescein kit (Eurogentec) according to the manufacturer's protocol and run on the iCycler iQ detection system (Bio-Rad SA, Marnes-la-Coquette, France) with the following thermal profile: an initial step of 3 min at 95 °C, followed by 40 cycles each consisting of 15 s at 95 °C and 1 min at 60 °C in a volume of 25 μ L. PCR products were checked by monitoring melting curves. For data analysis, the fluorescent signals were normalized using the reference gene, LDHA. Relative quantification, following the $\Delta\Delta$ Ct method⁴⁶ was applied to compare amounts of mRNA in healthy and dystrophic muscles. The average of gene level ratios in healthy conditions was normalized to 1. The average of gene level ratios in dystrophic muscles was expressed relatively to healthy conditions. Then, for each target gene, a statistical analysis was performed using Student's *t* test between healthy and dystrophic conditions.

Gene Ontology Annotation

Proteins identified as deregulated by the ICAT analyses were annotated using terms from the Gene Ontology (GO).⁴⁷ ENSEMBL protein identifiers, validated output from SEQUEST, were mapped to NCBI RefSeq identifiers and then to their corresponding Entrez Gene identifiers.⁴⁸ Because of the lack of systematic functional annotation for dog proteins, the annotations were transferred from the corresponding human orthologs, as determined by using the Homologene database.⁴⁹

RESULTS

In this study, the GRMD dog model was used to profile changes in protein abundance associated with DMD. Histological analysis of a 4-month old GRMD dog based on H&E staining revealed classical pathological changes of DMD including fiber size variation, fiber splitting, and central nucleation (Figure 1). Given the importance of protein phosphorylation in signaling pathways, it is not surprising that dysregulation of protein kinases and phosphatases had been linked to a vast number of pathologies, including neuromuscular disorders. To eliminate the structural and contractile proteins that are overabundant in crude protein extracts prepared from skeletal muscle, and to enrich the samples for signaling proteins,^{19,50} we restricted our analysis to the cytosolic and phospho-enriched proteins. A proteomic study,

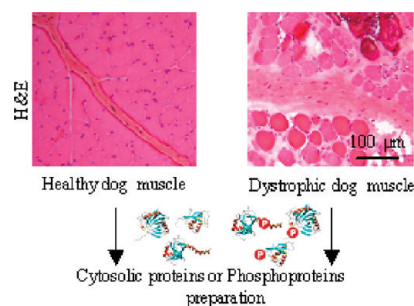


Figure 1. H&E (hematoxylin and eosin) staining showing classical pathological changes of DMD, including fiber size variation, fiber splitting, and central nucleation in skeletal muscle.

consisting of isotope-coded affinity tagging, was conducted separately on these two fractions.

Quantitative Analysis of Dystrophic Muscle Protein Profile Using cICAT Technology

To identify global protein perturbations present in GRMD dog muscle, cytosolic and phosphoprotein-enriched protein extracts from dystrophic and healthy muscles were prepared, labeled with cICAT reagents (¹²C₉ and ¹³C₉), and submitted to cICAT-MS/MS analysis. From the cytosolic extracts, 337 unique cICAT-labeled peptides were identified. After database searching (SEQUEST⁴⁰), validation (PeptideProphet & ProteinProphet⁵¹), and quantification (ASAP⁴⁴) followed by manual correction, a total of 88 cytosolic proteins were identified with a probability higher than 0.9 of being true positives (Supplementary Tables 1a and 2). Among these, 61 appeared to be differentially expressed in dystrophic muscle, with 30 proteins being overrepresented (Table 1a) and 31 underrepresented (Table 2a). The experiment with the phosphoprotein-enriched fractions led to the identification of a total of 122 unique peptides, corresponding to 63 different proteins, of which 40 had not been identified in the cytosolic extract (see Supplementary Tables 1b and 3 for additional details). Among these 63 proteins, 36 display quantitative changes in the dystrophic muscle, with 18 being overrepresented (Table 1b) and 18 being underrepresented (Table 2b) compared to healthy muscle. The PhosphoProtein Purification Kit enables a separation of the phosphorylated from the nonphosphorylated protein fraction. The affinity chromatography procedure reduces sample complexity and greatly facilitates analyses of low-abundance proteins. The experiment performed with the phospho-enriched samples led to the identification of 36 proteins differentially regulated between healthy and GRMD muscles (Tables 1b and 2b). Among these proteins, 31 had been previously described as phosphoproteins (Swiss-Prot and PhosphoSite databases), giving a good indication of the efficiency and the reliability of the purification method applied. For the other five, CSRP3, MYBPH, MYL6B, CYC1, CA3, no information relative to phosphorylation have been reported to date. It should be noted that a quantitative changes in the phospho-enriched fractions can result either from a difference in the amount of a protein or in its phosphorylation status.

Interestingly, 5 proteins identified by ICAT were also detected by 2-D/MS approach (Supplemental Figure 1). Moreover, among the proteins identified in the ICAT experiment, 6 were chosen for an analysis by Western immunoblot: LDHA, COF-2, DJ-1 (PARK7), PKM2, TUB and PP1 (Figure 2A,B). These six proteins displayed expression patterns similar to the ICAT ratios

Table 1. Overrepresented Proteins in Dystrophic versus Healthy Dog Muscle Protein Extract^a

symbol	protein name	log2 ratio GRMD/Healthy
(a) Cytosolic Protein Sample		
MTPN	Myotrophin	Only detected in GRMD sample
TPM4	Tropomyosin 4	Only detected in GRMD sample
CKMT2	Creatine kinase, mitochondrial 2	3.06
A1AG1	similar to Alpha-1 acid glycoprotein	2.25
CSRP3	Cysteine and glycine-rich protein 3	1.72
CLIC4	Chloride intracellular channel 4	1.66
A1BG	Alpha-1-B glycoprotein	1.43
AHSG	Alpha-2-HS-glycoprotein	1.33
HSP90AA4P	Putative heat shock protein HSP 90-alpha A4	1.28
GSTP1	Glutathione S-transferase PI isozyme YD1-2YD1-2(IV-HB)	1.24
ANP32A	Acidic leucine-rich nuclear phosphoprotein 32 family	1.19
ALB	Serum albumin (allergen Can f 3)	1.10
CALR	Calreticulin	1.06
FETUB	Fetuin B	1.06
TUBA2	similar to tubulin, alpha 2 isoform 2	1.06
PDLIM3	PDZ and LIM domain 3	1.02
ANXA1	Annexin I	0.94
HPX	Hemopexin	0.90
ACTC	Cardiac actin	0.90
TPM2	Tropomyosin beta chain (Tropomyosin-2)	0.83
LGALS1	Lectin, galactoside-binding, soluble, 1 (galectin 1)	0.83
GOT1	aspartate aminotransferase 1	0.76
PLIN4	perilipin 4	0.76
MYL1	Myosin, light chain 1, alkali; skeletal, fast	0.76
ANXA2	Annexin A2	0.66
PFN1	profilin 1	0.63
TTN	Cardiac titin	0.63
PP1	Serine/threonine-protein phosphatase PP1-beta catalytic subunit	0.60
PGAM2	Phosphoglycerate mutase 2 (muscle)	0.57
TUBB2C	Tubulin, beta 2C	0.54
(b) Phospho-Enriched Protein Sample		
TPM4	* Tropomyosin 4	Only detected in GRMD sample
MYL3	Myosin, light chain 3, alkali; ventricular, skeletal, slow	2.82
VIM	Vimentin-like protein	2.06
TUBB6	Tubulin, beta 6	1.66
TUBB2C	* Tubulin, beta 2C	1.52
LGALS1	* Lectin, galactoside-binding, soluble, 1 (galectin 1)	1.39
ALB	* Serum albumin (allergen Can f 3)	1.35
PCYT1A	Phosphate cytidyltransferase 1, choline, alpha	1.12
CSRP3	* Cysteine and glycine-rich protein 3 (cardiac LIM protein)	1.12
MYBPH	Myosin binding protein H	0.99
MYH3	Developmental myosin heavy chain embryonic	0.96
TUBA2	* similar to tubulin, alpha 2 isoform 2	0.87
MYPN	Myopalladin	0.84
PTGES3	Prostaglandin E synthase 3 (cytosolic)	0.84
TPM2	Tropomyosin beta chain (Tropomyosin-2)	0.76
EEF1B2	Eukaryotic translation elongation factor 1 beta 2	0.68
MYL6B	Myosin, light chain 6B	0.66
BIN1	Bridging integrator 1	0.66

^a Proteins were identified by ICAT-MS/MS in two experiments using *vastus lateralis* muscle from 4 month-old healthy and GRMD dogs. Two different experiments were performed, one with the cytosolic fraction (Healthy dog#1; GRMD dog#1: Table 1a), and the other one with a phospho-enriched protein sample (Healthy dog#2; GRMD dog#2: Table 1b). Shown here are the centered log2 ASAP ratios (GRMD/Healthy) of the 48 proteins (30 for the cytosolic protein sample and 18 for the phospho-enriched protein sample) that display changes in their abundance between healthy and dystrophic muscle. Asterisks (*) denote proteins identified in both experiment (cytosolic and phospho-protein enriched fractions). GRMD, Golden Retriever Muscular Dystrophy.

Table 2. Underrepresented Proteins in Dystrophic versus Healthy Dog Muscle^a

symbol	name	log ₂ ratio GRMD/Healthy
(a) Cytosolic Protein Sample		
PGK1	Phosphoglycerate kinase 1	-0.61
ACADS	Acyl-Coenzyme A dehydrogenase, C-2 to C-3 short chain	-0.62
ENO3	Enolase 3 (beta, muscle)	-0.70
GAPDH	Glyceraldehyde-3-phosphate dehydrogenase (GAPDH) (EC 1.2.1.12)	-0.70
ACO2	Aconitase 2, mitochondrial	-0.72
MYH3	Developmental myosin heavy chain embryonic	-0.72
UQCRC1	Ubiquinol-cytochrome c reductase core protein I	-0.74
ALDOA	Aldolase A	-0.74
ACADVL	Acyl-Coenzyme A dehydrogenase, very long chain	-0.77
MYH2	Myosin-2 (Myosin heavy chain 2)	-0.77
MYH7	Myosin-7 (Myosin heavy chain 7)	-0.77
MYH8	Myosin-8 (Myosin heavy chain 8)	-0.77
PGM1	Phosphoglucomutase 1	-0.79
CA3	Carbonic anhydrase III, muscle specific	-0.86
FABP4	Fatty acid binding protein 4, adipocyte	-0.88
FABP3	Fatty acid binding protein 3, muscle and heart	-0.92
MDH2	Malate dehydrogenase (EC 1.1.1.37)	-0.95
AK1	Adenylate kinase 1	-0.97
PRDX3	Peroxiredoxin 3	-1.00
PARK7	Parkinson disease (autosomal recessive, early onset) 7	-1.06
UQCRH	Ubiquinol-cytochrome c reductase hinge protein	-1.07
HSPB6	Heat shock protein, alpha-Crystallin-related. B6	-1.11
ATP2A2	Sarcoplasmic/endoplasmic reticulum calcium ATPase 2	-1.16
ATP5A1	similar to ATP synthase alpha chain, mitochondrial precursor	-1.19
MYLPF	Myosin regulatory light chain 2, skeletal muscle isoform	-1.22
GOT2	aspartate aminotransferase 2	-1.38
VDAC1	voltage-dependent anion channel 1	-1.51
CAMK2D	Calcium/calmodulin-dependent protein kinase (CaM kinase) II delta	-1.99
CKM	Creatine kinase M-type	-2.05
HP	Haptoglobin	-2.76
PFKM	6-phosphofructokinase, muscle type (Phosphofructokinase 1)	Only detected in Healthy sample
(b) Phospho-Enriched Protein Sample		
PSMA3	Proteasome (prosome, macropain) subunit, alpha type, 3	-0.56
FLNC	* Filamin C, gamma (actin binding protein 280)	-0.60
CYC1	Cytochrome c-1	-0.61
CA3	* Carbonic anhydrase III, muscle specific	-0.62
TOMM70A	Translocase of outer mitochondrial membrane 70 homologue	-0.63
PRKAR2A	Protein kinase, cAMP-dependent, regulatory, type II, alpha	-0.79
ATP2A1	ATPase, Ca ⁺⁺ transporting, cardiac muscle, fast twitch 1	-0.80
PFKM	* 6-phosphofructokinase, muscle type (Phosphofructokinase 1)	-1.02
PRKAR1A	Protein kinase, cAMP-dependent, regulatory, type I, alpha	-1.15
MYH2	* Myosin-2	-1.21
ENO1	ENO1 enolase 1	-1.36
CKM	* Creatine kinase M-type	-1.47
PDHB	Pyruvate dehydrogenase (lipoamide) beta	-1.54
UQCRC1	* Ubiquinol-cytochrome c reductase core protein I	-1.59
MYOM3	Myomesin-3	-1.82
MYOT	Myotilin (Titin immunoglobulin domain protein)	-1.85
CFL2	Cofilin 2	-2.64
AMPD2	adenosine monophosphate deaminase 2	Only detected in Healthy sample

^a Proteins were identified by ICAT-MS/MS in two experiments using *vastus lateralis* muscle from 4-month old healthy and GRMD dogs. Two different experiments were performed, one with the cytosolic fraction (Healthy dog#1; GRMD dog#1: Table 2a), and the other one with a phospho-enriched protein sample (Healthy dog#1; GRMD dog#1: Table 2b). Shown here are the centered log₂ ASAP ratios (GRMD/Healthy) of the 49 identified proteins (31 in the cytosolic protein sample and 18 in the phospho-enriched protein sample) that display abundance changes between healthy and dystrophic muscle. Asterisks (*) denote proteins identified in both experiment (in the cytosolic and in the phospho-protein enriched fractions). GRMD, Golden Retriever Muscular Dystrophy.

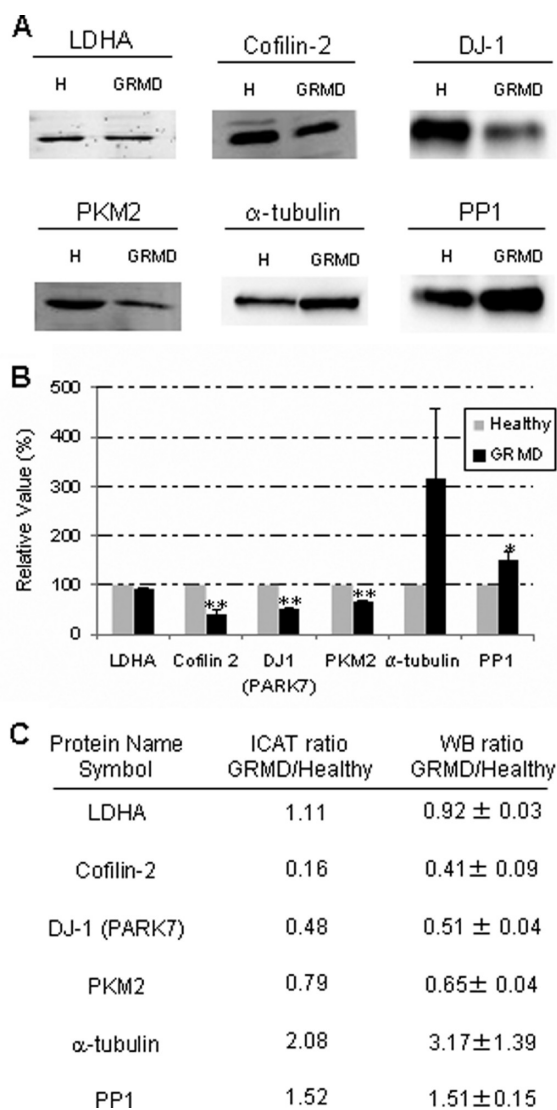


Figure 2. (A) Western immunoblot analyses. Representative images of immunoblots have been shown. Cytosolic proteins were separated by SDS-PAGE and the blotted proteins were revealed with specific antibodies. The results obtained confirm the increased expression level detected in dystrophic muscle for PP1 and the α -tubulin, and the decreased expression level detected for cofilin 2 and DJ-1 (no significant difference for LDHA and a low decreased expression for PKM2). H, healthy; GRMD, Golden Retriever Muscular Dystrophy. (B) Graphical representation of the immunoblot analysis of proteins in dystrophic tissue. The histogram represents the relative level of LDHA, Cofilin 2, DJ-1, PKM2, α -tubulin, and PP1 in healthy and GRMD *vastus lateralis* muscle. The mean variation ($n = 3$) was calculated and the GRMD value was represented as a percentage of the healthy level taken as 100%; Statistical significance from *t* test analysis (StatEL software; Excel, Microsoft): * $p < 0.05$; ** $p < 0.02$ vs healthy conditions. (C) Quantitative MS and Western blot data Comparison of ICAT ratio and quantification of proteins described by Western blotting experiment.

(Figure 2C). Indeed, we could confirm that PP1 and the tubulin α are overrepresented in dystrophic muscle, and that cofilin 2 and DJ-1 (PARK7) are underrepresented, while the level of LDHA remains similar between the two samples. In addition, we also confirmed by Western blot that PKM2, a protein with a ICAT log₂ ratio (GRMD/Healthy) of -0.33 (ICAT and Western blot ratios GRMD/Healthy, respectively, 0.79 and 0.65) is

detected at lower levels in GRMD muscle (Supplemental Table 1a,b, and Figure 2). While we have chosen a stringent cutoff of log₂ ratio ± 0.5 to identify proteins that are differentially represented in dystrophic muscle, proteins described in Tables 1 and 2 can be considered as potential candidates for quantitative changes between healthy and GRMD muscle.

Functional Annotation Analysis of Protein Changes between Healthy and Dystrophic Muscles

Proteins that are differentially represented between healthy and dystrophic muscle were grouped in functional classes according to the Gene Ontology (GO) terms of their human homologues according to "biological process" categories (Table 3). A background list of nonchanging proteins is presented in Supplementary Table 4. Through this functional annotation, the 84 proteins identified as significantly dysregulated in dystrophic muscle by the ICAT experiments (namely 61 proteins from the cytosolic fraction and 36 proteins from the phospho-enriched fraction, with an overlap of 13 proteins) were classified into 7 major categories including: (i) muscle development and contraction (31), (ii) glycolytic metabolism (14), (iii) oxidative metabolism (19), (iv) calcium ion homeostasis (6), (v) intracellular signaling (12), (vi) regulation of apoptosis (13), and (vii) other functions (15). GO annotation of the altered proteome led to several key findings which might reflect ongoing muscle regeneration taking place within dystrophic muscle. Importantly, our quantitative study using healthy and dystrophic samples allowed us to reveal important changes in the abundance of key proteins involved in these major metabolic pathways. The list of the GO categories obtained was similar to the list found in a study concerning the characterization of the human skeletal muscle proteome.⁵² In this study, the authors identified all the enzymes participating in the major pathways of glucose and lipid metabolisms, a large number of proteins involved in mitochondrial oxidative phosphorylation and calcium homeostasis, and isoforms of the proteins that constitute the myofibrillar apparatus.

We detected a number of cytoskeletal microtubules components as being overrepresented in dystrophic muscle, such as myosin light chains (MYL6B, MYL1, MYL3). Other muscle structure and regeneration proteins were also overrepresented including tubulin, tropomyosin, filamin, and titin (Table 3). Our study identified 5 key proteins of the glycolytic metabolic pathway as being underrepresented in dystrophic muscle: the pyruvate dehydrogenase, the phosphoglycerate kinase, the phosphoglucomutase, the enolase and the adenylate kinase (Table 3). Moreover, we identified alterations in the level of several proteins involved in Ca²⁺ homeostasis (Table 3). The ATPase Ca²⁺ transporting protein (ATP2A2) appeared underrepresented in dystrophic muscle, while proteins involved in Ca²⁺ translocation from the cytosol to the sarcoplasmic reticulum, and in Ca²⁺ homeostasis during muscle contraction, were found to be overrepresented (namely, chloride intracellular channel, calcium/calmodulin-dependent protein kinase and calreticulin) (Table 3). In addition, we observed an increased level of annexins A1 and A2 in healthy muscle (Table 3), suggesting a possible pathogenic contribution of these calcium-binding proteins.

Among the 12 proteins that are altered in dystrophic muscle and involved in intracellular signaling (Table 3), the protein phosphatase 1 (PP1) and the Parkinson's disease protein, DJ-1 (PARK7) appear particularly interesting. The PP1 phosphatase,

Table 3. Classification of the Proteins Identified by ICAT as Differentially Represented in the Healthy and Dystrophic Dog *Vastus Lateralis* Muscles, According to Their “Biological Process” GO Terms^a

GO term biological process	lower expression in GRMD dog		higher expression in GRMD dog	
	cytosolic fraction	phospho-enriched fraction	cytosolic fraction	phospho-enriched fraction
muscle development and contraction	ALDOA, CAMK2D, MYH2, MYH7, MYH8, MYH3, MYLPF, CA3	ATP2A1, CA3, CFL2, FLNC, MYH2, MYOT,	ACTC, CKMT2, CSRP3, MYL1, PDLIM3, PFN1, PGAM2, TPM2, TPM4, TTN, TUBA2, TUBB2C	BIN1, CSRP3, MYBPH, MYH3, MYL3, MYL6B, MYPN, TPM2, TPM4, TUBB6, TUBB2C, TUBA2, VIM
glycolytic metabolism	ALDOA, AK1, CKM, ENO3, GAPDH, MDH2, PFKM, PCK1, PGMI, AK1,	CKM, ENO1, PDHB, PFKM	PGAM2, PP1	
oxidative metabolism	ACADS, ACADVL, GAPDH, MDH2, PARK7, PRDX3, UQCRC1, UQCRC1, ACO2, ALDOA, ATP5A1, FABP3, FABP4	CYC-1, PDHB, PRKARIA, PRKAR2A, UQCRC1	PGAM2, PP1	
calcium ion homeostasis	ATP2A2, CAMK2	ATP2A1	CALR, CSRP3, CLIC4	CSRP3
intracellular signaling	ATP2A2, PARR7	PRKARIA, PRKAR2A	ANP32A, CALR, HPX, LGALS1, TTN, PPI, AHSG, FETUB	LGALS1
regulation of apoptosis	HSPB6, PRDX3, VDAC1,	ATP2A1	ACTC, ALB, ANXA1, ANXA2, CALR, GSTP1, LGALS1, HSP90, TUBB2C	ALB, LGALS1, TUBB2C
Other	GOT2, HP, NDUFB1	AMPD2, PSMA3, TOMM70A,	MTPN, AIAG1, AIBG, AHSG, GOT1, PLIN4	PCYT1A, PTGES3, EEF1B2,

^a Through this functional annotation, the 84 proteins identified as significantly dysregulated in dystrophic muscle by the ICAT experiments (namely 61 proteins from the cytosolic fraction and 36 proteins from the phospho-enriched fraction, with an overlap of 13 proteins) were classified into 7 major categories. A large proportion of these dysregulated proteins belong to muscle development and muscle metabolism including glycolytic and oxidative elements.

present in skeletal muscle, is activated by the glycogen synthase kinase 3 (GSK3 β) and DJ-1 has been recently described as a regulator of the tumor suppressor PTEN.^{53,54} The ICAT experiment revealed a higher abundance of PP1 in dystrophic muscle that could be confirmed by Western immunoblot analysis (Table 3, Figure 2). The drastic underrepresentation of DJ-1 detected by ICAT was later confirmed by Western immunoblot analysis (Table 3, Figure 2).

Decreased Protein Level and Altered Transcriptional Regulation of PGC-1 α Targets

Interestingly, 30% of the proteins we found underrepresented in dystrophic muscle are coded by genes reported to be induced by the peroxisome proliferator-activated receptor-gamma coactivator-1 alpha (PGC-1 α) in murine myoblasts⁵⁵ (data compiled from the Molecular Signature Database⁵⁶) (Figure 3A). In the same study,⁵⁵ a modest reduction in the expression of PGC-1 α in diabetic muscle was shown to be responsible for the mitochondrial deregulation observed in diabetes. Next, our hypothesis of an altered transcriptional regulation of PGC-1 α and its downstream putative targets in dystrophic dog muscle was investigated by real-time RT-PCR. The expression of PGC-1 α gene and of 4 downstream putative targets genes (ACADS, FABP3, CYC1 and PFKM) randomly chosen in the list of PGC-1 α targets down-regulated at the protein level (Table 2, Figure 3A) were analyzed in RNA extracts from healthy and dystrophic dog muscles. As shown in Figure 3B, the down-expression of the PGC-1 α gene (0.54 ± 0.08 , $p = 0.010$) and its four target genes, ACADS (0.63 ± 0.17 , $p = 0.059$), FABP3 (0.42 ± 0.10 , $p = 0.004$), CYC1 (0.53 ± 0.11 , $p = 0.011$) and PFKM (0.48 ± 0.18 , $p = 0.039$) is significantly validated.

This suggested to us that PGC-1 α might as well be down-regulated in the dystrophic dog muscle. To test this hypothesis, we chose to perform an immunofluorescence experiment because of the low basal levels of this protein. In healthy dog muscle section, PGC-1 α labeling was observed in subsarcolemmal as well as endomysial nuclei. In dystrophic muscle, the same expression profile was observed albeit with a lower intensity (Figure 3C), confirming that the PGC-1 α protein is underrepresented in dystrophic muscle. The immunolocalization data (Figure 3C) show that hypertrophied and large fibers do not display subsarcolemmal expression for PGC-1 α . This label seems to concern cluster of small fibers.

Taken together, these results strongly indicate that the decreased protein levels of PGC-1 α and of its downstream targets in dystrophic muscles arise from a transcriptional alteration (Figure 3). This alteration could play an important role in DMD and, as such, might represent a potential therapeutic target.^{35,57,58}

DISCUSSION

The precise molecular mechanisms that define the pathogenesis of DMD are not yet fully understood, hampering the development of palliative treatments and interventions that may slow down disease progression. In this perspective, high-throughput technologies, such as microarray-based gene expression profiling, have been recently applied to human biopsies.^{52,59,60} These studies revealed that the expression level of genes involved in key metabolic pathways differ significantly between healthy and DMD muscles (105 and 618 genes were, respectively, identified). On the other hand, proteomic studies performed during the past few years have demonstrated that

mass-spectrometry-based technologies can be employed to study skeletal muscle proteins. Recently, 1D-gel electrophoresis and HPLC-ESI-MS/MS was used to characterize the proteome of healthy human skeletal muscle.⁵² This study provides the most comprehensive proteome coverage of human skeletal muscle. Protein expression profiling thus appears as an effective approach to define the biochemical cascades that underlie the progressive pathophysiology of DMD. The proteomic analysis that we performed using the clinically relevant GRMD dog model indeed allowed us to gain additional insight into the biochemical basis of the disease. Of the 127 proteins identified in the present study using *vastus lateralis* canine muscle, 101 were also detected in the Hojlund study.⁵² Studies using 2D-gel electrophoresis and MS had already been applied to the proteomic profiling of young and aged *mdx* versus healthy skeletal muscle and diaphragm.^{22,24,31} The proteomics findings resulting from these studies support the pathobiochemical concept that deficiency in dystrophin results in abnormalities in glycolysis, fatty acid oxidation and ion homeostasis pathways. Many proteins involved in mitochondrial function and energy metabolism were found to be altered. Of interest, our data indicated that several proteins such as adenylate kinase, PP1 phosphatase, annexin, carbonic anhydrase, and aldolase were also differentially expressed in dystrophic versus healthy dog muscle, suggesting that generalized mitochondrial dysfunction and metabolism crisis are a characteristic common to dystrophic muscles from different animal model. More recently, the combination of proteomics, metabolomics, and fluxomics has confirmed the existence in the *mdx* mouse model of DMD of perturbations that reflect mitochondrial energetic alterations.⁶¹ The broad aim of these studies has been twofold, first the identification of cofounding factors that promote or limit the disease progression and second, the identification of new biomarkers that could be used to more accurately define disease status. Our study is in keeping with this perspective, and the results obtained are discussed in details hereafter.

Glycolytic and Oxidative Metabolism

The most striking observation made during this study was the dramatic alteration of metabolic proteins in dystrophic dog muscle. Several key enzymes of energy metabolism appeared underrepresented in dystrophic versus healthy dog muscle, including proteins that control both glycolytic and oxidative metabolism. The altered glycolytic enzymes included adenylate kinase, a change previously noted in the *mdx* mouse model⁶² and in human patients.⁶³ Nevertheless, the most profound alterations were noted for a cohort of mitochondrial proteins, which again reinforces the concept that basal metabolic function is perturbed in the dystrophic muscle environment. In an interesting manner, it has been estimated that 22% of the proteins detected in human skeletal muscle could be attributed to the mitochondrion⁵² and decreased energy production, mitochondrial swelling, and abnormalities were described as a secondary feature of muscular dystrophy in the *mdx* mouse model.^{64,65}

Among the 45 proteins that we identified as underrepresented in dystrophic dog muscle (4 proteins are identified in both cytosolic and phospho-enriched protein samples), 13 has been described as regulated at the transcriptional level by the co-activator PGC-1 α (Figure 3A and ref 56). We were able to show that PGC-1 α itself was present at a lower level in dystrophic dog muscle, strongly suggesting that the reduction in the PGC-1 α -regulated transcriptome may originate from a reduction in its expression level (Figure 3C). Of interest, among the PGC-1 α

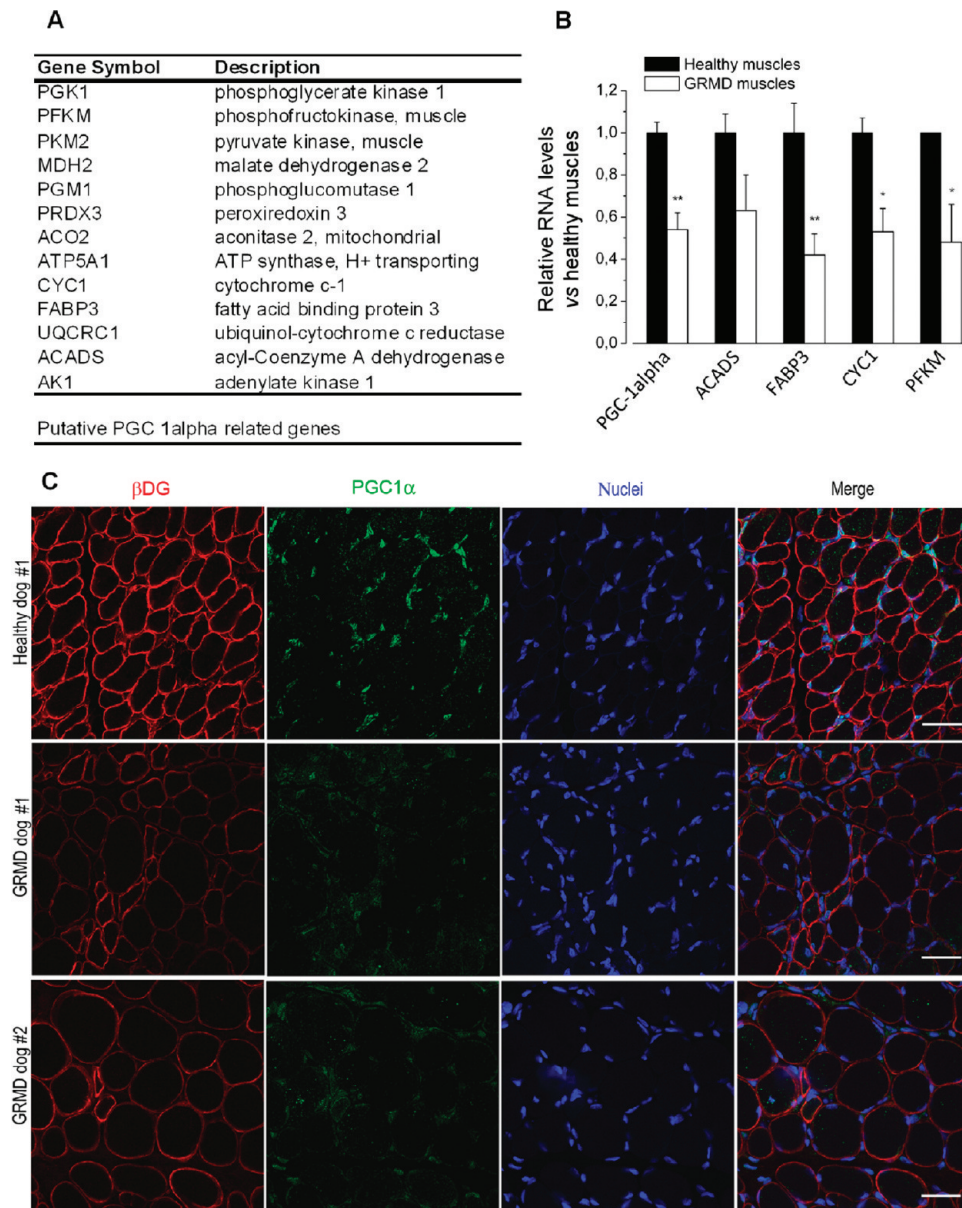


Figure 3. Decrease protein level and altered transcriptional regulation of PGC-1 α targets in GRMD dog muscle. (A) Set of proteins underrepresented in dystrophic muscle identified as PGC-1 α targets. (B) Relative level of PGC-1 α gene and of selected target genes in healthy and dystrophic dog muscles by quantitative RT-PCR. Data are means \pm SEM of 2 individual healthy and 3 individual GRMD dogs. Statistical significance from *t* test analysis: **p* < 0.05; ***p* < 0.01 vs healthy conditions. The LDHA gene was used as an internal reference gene. (C) Immunofluorescence analysis of PGC-1 α for muscle sections from healthy and GRMD dogs. β -Dystroglycan, plasma membrane marker (red fluorescence); PGC-1 α (green fluorescence); nuclei stained (blue fluorescence); and merge. Scale bar: 40 μ m. A strong fluorescent labeling is visible in healthy muscle at the periphery of muscle fibers, whereas a fall in the intensity for PGC-1 α staining was observed in the dystrophic dogs sample.

targets that we identified as underrepresented in dystrophic dog muscle (Figure 3A), 5 (namely, PFKM, PGM1, ACO2, CYC1, and FABP3) had already been identified in a transcriptomic study as expressed at lower level in DMD versus healthy human biopsies.⁶⁰ PGC-1 α has been described as a potent regulator of mitochondrial biogenesis and oxidative metabolism in skeletal muscle.^{66,67} In addition, activation of the peroxisome proliferator-activated receptor (PPAR)/PGC-1 α pathway has been shown, by preventing the bioenergetic deficit observed, to efficiently improve a mitochondrial myopathy phenotype,⁶⁸ suggesting that PGC-1 α mediated improvement of dystrophic muscle may rely (in part) on the restoration of PGC-1 α mitochondrial targets.⁶⁹

Interestingly, a recent study has shown that pharmacologic activation of peroxisome proliferator-activated receptor (PPAR) β/δ also leads to an upregulation in the expression of utrophin A, which was concurrent with a partial correction of the dystrophic phenotype.⁷⁰ As such, enhancing the expression of PGC-1 α may present a multilevel advantage to improve the dystrophic muscle phenotype.

Calcium Signaling and Trafficking

We found that a number of proteins involved in Ca²⁺ translocation and homeostasis, namely, chloride intracellular channel, calcium/calmodulin-dependent protein kinase, and

calreticulin as well as some forms of annexins were overrepresented in dystrophic versus healthy dog muscle (Table 3). The increased expression of calcium-handling proteins is likely to be a compensatory response to the altered calcium dynamics observed in dystrophic muscle fibers. Indeed, when dystrophin is absent from muscle, a natural membrane resealing process occurs; Ca^{2+} leak channels are introduced into the sarcolemma, causing an elevation of cytosolic Ca^{2+} .²³ The elevation of proteins involved in calcium homeostasis and trafficking observed in dystrophic dog muscle could be part of this mechanism. As far as the annexins are concerned, a study performed in the mouse model of dysferlinopathy, another muscular pathology that includes the Limb Girdle Muscular Dystrophy type 2B, had already shown that annexin A1 and A2 interact with dysferlin and the proteins had been described as potential muscular dystrophy genes.⁷¹ Annexins form a diverse family of Ca^{2+} -dependent phospholipid binding proteins widely distributed that are involved in a variety of processes, including membrane scaffolding, trafficking and organization of vesicles, exocytosis, endocytosis, and calcium ion channel formation. The increased level of annexins detected in dystrophic versus healthy dog muscle may reflect an adaptation to the altered calcium concentrations and the continual sarcolemmal disruptions observed in these circumstances.

Intracellular Signaling

Lastly, we identified alterations in a number of key signaling proteins in dystrophic muscle. Notably, our ICAT analysis revealed a strong increase in the level of the PP1 protein in dystrophic dog muscle, which was confirmed by Western immunoblot (Table 1 and Figure 2). In skeletal muscle, PP1 is known to regulate both glycogen and fatty metabolism,⁷² while promoting the dephosphorylation of myosin.⁷³ Interestingly, a constitutive activation of PP1 had been reported previously in *mdx* skeletal muscle, and attributed to the enhanced protein turnover that occurs during ongoing muscle damage,^{31,54} suggesting that the increased level of PP1 that we also observed in dystrophic dog muscle may represent a conserved feature in DMD animal model. We also detected a drastic underrepresentation of the DJ-1 protein in dystrophic versus healthy dog muscle (also called PARK7). This Parkinson's disease-associated protein was recently described as a negative regulator of the tumor suppressor PTEN, a phosphatase involved in the regulation of the PI3K/Akt pathway.⁵³ In a previous study,¹⁹ we showed that PTEN is overrepresented and more active in dystrophic versus healthy dog muscle, leading to a decreased phosphorylation of Akt and the downstream kinases GSK3 β and p70S6K. Other studies performed in the *mdx* mouse model and in human biopsies had already described an alteration of the PI3K/Akt signaling pathway in the dystrophic muscle,^{17,74,75} and it has been shown that increasing Akt activity by transgenic overexpression of the activated kinase itself can reverse the dystrophic phenotype.^{20,76} Given the role of DJ-1 in the regulation of the PTEN phosphatase, the results presented here suggest that PTEN activation in dystrophic dog muscle may originate from the underexpression of DJ-1. Noteworthy, in addition to its role in PTEN's regulation, DJ-1 also promotes the activity of PGC-1 α .⁷⁷ As such, DJ-1 sensitive signaling pathways may provide high priority targets for the development of novel drug therapies for DMD.

Summary

We used the ICAT/MS technology to map and identify clinically relevant alterations in the proteomic signature of dystrophic dog muscle. We were able to identify differences in

the representation of key proteins between healthy and GRMD skeletal muscles, supporting the hypothesis that secondary changes may play an active role in muscular dystrophy. Our observations provide the first evidence of a dysregulation of the co-activator PGC-1 α in dystrophic dog muscle, an alteration that may be at the origin of the general metabolic crisis that characterizes the disease. Taken together, these results suggest that the restoration of metabolic control may offer a novel treatment regime to attenuate dystrophic muscle damage.

■ ASSOCIATED CONTENT

Supporting Information

Supplementary tables and figures. This material is available free of charge via the Internet at <http://pubs.acs.org>.

■ AUTHOR INFORMATION

Corresponding Author

*Laetitia Guevel, CNRS UMR6204, Faculté des Sciences et des Techniques, Université de Nantes, F-44322 Nantes Cedex 3, France. Phone, +33-251125622; fax, +33-251125637; e-mail, laetitia.guevel@univ-nantes.fr.

Author Contributions

*J.R.L. and C.P.-I. contributed equally to this work. M.B. and L.A.M. share equal contribution as senior authors.

■ ACKNOWLEDGMENT

We gratefully acknowledge Dr. Lawrence Puente, from the Stem Core Facility for his technical support, Gareth Palidwor for bioinformatics support on the TPP and Gwenina Cuff for technical assistance in mRNA extraction. This work was supported by funding from the AFM (Association Française contre les Myopathies), No. 14033 to L.G. and by funding from The Muscular Dystrophy Association USA to L.A.M. L.A.M. holds the Mach-Gaensslen Chair in Cardiac Research. M.B. holds the Canadian Research Chair in the Regulation of Gene Expression.

■ ABBREVIATIONS

ACN, acetonitrile; BCA, bicinchoninic acid; DGC, dystrophin–glycoprotein complex; DMD, Duchenne muscular dystrophy; ESI, electrospray ionization; GO, Gene Ontology; GRMD, Golden Retriever Muscular Dystrophy; cICAT, cleavable isotope-coded affinity tag; ICAT/MS/MS, isotope-coded affinity tag/tandem mass spectrometry; LTQ, ion trap mass spectrometer; MAPK, mitogen-activated protein kinase; *mdx*, X-linked muscular dystrophy; MS, mass spectrometry; PI3K, phosphatidylinositol 3-kinase; PP1, protein phosphatase 1; SCX, strong cation exchange; SDS-PAGE, sodium dodecyl sulfate polyacrylamide gel electrophoresis; TCA, trichloroacetic acid; TFA, trifluoroacetic acid; TPP, Trans-Proteomic Pipeline.

■ REFERENCES

- (1) Emery, A. *Duchenne Muscular Dystrophy*; Oxford University Press: Oxford, 1993; Vol. 24.
- (2) Hoffman, E. P.; Brown, R. H., Jr.; Kunkel, L. M. Dystrophin: the protein product of the Duchenne muscular dystrophy locus. *Cell* **1987**, *51* (6), 919–928.
- (3) Koenig, M.; Hoffman, E. P.; Bertelson, C. J.; Monaco, A. P.; Feener, C.; Kunkel, L. M. Complete cloning of the Duchenne muscular

dystrophy (DMD) cDNA and preliminary genomic organization of the DMD gene in normal and affected individuals. *Cell* **1987**, *50* (3), 509–517.

(4) Monaco, A. P.; Neve, R. L.; Colletti-Feener, C.; Bertelson, C. J.; Kurnit, D. M.; Kunkel, L. M. Isolation of candidate cDNAs for portions of the Duchenne muscular dystrophy gene. *Nature* **1986**, *323*, 646–650.

(5) Campbell, K. P.; Kahl, S. D. Association of dystrophin and an integral membrane glycoprotein. *Nature* **1989**, *338* (6212), 259–262.

(6) Ervasti, J. M.; Ohlendieck, K.; Kahl, S. D.; Gaver, M. G.; Campbell, K. P. Deficiency of a glycoprotein component of the dystrophin complex in dystrophic muscle. *Nature* **1990**, *345* (6273), 315–319.

(7) Ibraghimov-Beskrovnaya, O.; Ervasti, J. M.; Leveille, C. J.; Slaughter, C. A.; Sernett, S. W.; Campbell, K. P. Primary structure of dystrophin-associated glycoproteins linking dystrophin to the extracellular matrix. *Nature* **1992**, *355* (6362), 696–702.

(8) Yoshida, M.; Ozawa, E. Glycoprotein complex anchoring dystrophin to sarcolemma. *J. Biochem. (Tokyo)* **1990**, *108* (5), 748–752.

(9) Straub, V.; Campbell, K. P. Muscular dystrophies and the dystrophin-glycoprotein complex. *Curr. Opin. Neurol.* **1997**, *10* (2), 168–175.

(10) Straub, V.; Rafael, J. A.; Chamberlain, J. S.; Campbell, K. P. Animal models for muscular dystrophy show different patterns of sarcolemmal disruption. *J. Cell Biol.* **1997**, *139* (2), 375–385.

(11) Brenman, J. E.; Chao, D. S.; Gee, S. H.; McGee, A. W.; Craven, S. E.; Santillano, D. R.; Wu, Z.; Huang, F.; Xia, H.; Peters, M. F.; Froehner, S. C.; Bredt, D. S. Interaction of nitric oxide synthase with the postsynaptic density protein PSD-95 and alpha1-syntrophin mediated by PDZ domains. *Cell* **1996**, *84* (5), 757–767.

(12) Cavaldesi, M.; Macchia, G.; Barca, S.; Defilippi, P.; Tarone, G.; Petrucci, T. C. Association of the dystroglycan complex isolated from bovine brain synaptosomes with proteins involved in signal transduction. *J. Neurochem.* **1999**, *72* (4), 1648–1655.

(13) Crosbie, R. H.; Yamada, H.; Venzke, D. P.; Lisanti, M. P.; Campbell, K. P. Caveolin-3 is not an integral component of the dystrophin glycoprotein complex. *FEBS Lett.* **1998**, *427* (2), 279–282.

(14) Bulfield, G.; Siller, W. G.; Wight, P. A. G.; Moore, K. J. X chromosome-linked muscular dystrophy (mdx) in the mouse. *Proc. Natl. Acad. Sci. U.S.A.* **1984**, *81*, 1189–1192.

(15) Kolodziejczyk, S. M.; Walsh, G. S.; Balazsi, K.; Seale, P.; Sandoz, J.; Hierlihy, A. M.; Rudnicki, M. A.; Chamberlain, J. S.; Miller, F. D.; Megoney, L. A. Activation of JNK1 contributes to dystrophic muscle pathogenesis. *Curr. Biol.* **2001**, *11* (16), 1278–1282.

(16) Langenbach, K. J.; Rando, T. A. Inhibition of dystroglycan binding to laminin disrupts the PI3K/AKT pathway and survival signaling in muscle cells. *Muscle Nerve* **2002**, *26* (5), 644–653.

(17) Peter, A. K.; Crosbie, R. H. Hypertrophic response of Duchenne and limb-girdle muscular dystrophies is associated with activation of Akt pathway. *Exp. Cell Res.* **2006**, *312* (13), 2580–2591.

(18) St-Pierre, S. J.; Chakkalakal, J. V.; Kolodziejczyk, S. M.; Knudson, J. C.; Jasmin, B. J.; Megoney, L. A. Glucocorticoid treatment alleviates dystrophic myofiber pathology by activation of the calcineurin/NF-AT pathway. *FASEB J.* **2004**, *18* (15), 1937–1939.

(19) Feron, M.; Guevel, L.; Rouger, K.; Dubreil, L.; Arnaud, M. C.; Ledevin, M.; Megoney, L.; Cherel, Y.; Sakanyan, V. PTEN contributes to profound PI3K/Akt signaling pathway deregulation in Dystrophin-deficient dog muscle. *Am. J. Pathol.* **2009**, *174* (4), 1459–1470.

(20) Peter, A. K.; Ko, C. Y.; Kim, M. H.; Hsu, N.; Ouchi, N.; Rhie, S.; Izumiya, Y.; Zeng, L.; Walsh, K.; Crosbie, R. H. Myogenic Akt signaling upregulates the utrophin-glycoprotein complex and promotes sarcolemma stability in muscular dystrophy. *Hum. Mol. Genet.* **2009**, *18* (2), 318–327.

(21) Blaauw, B.; Mammucari, C.; Toniolo, L.; Agatea, L.; Abraham, R.; Sandri, M.; Reggiani, C.; Schiaffino, S. Akt activation prevents the force drop induced by eccentric contractions in dystrophin-deficient skeletal muscle. *Hum. Mol. Genet.* **2008**, *17* (23), 3686–3696.

(22) Doran, P.; Dowling, P.; Donoghue, P.; Buffini, M.; Ohlendieck, K. Reduced expression of regucalcin in young and aged mdx diaphragm indicates abnormal cytosolic calcium handling in dystrophin-deficient muscle. *Biochim. Biophys. Acta* **2006**, *1764* (4), 773–785.

(23) Doran, P.; Dowling, P.; Lohan, J.; McDonnell, K.; Poetsch, S.; Ohlendieck, K. Subproteomics analysis of Ca²⁺-binding proteins demonstrates decreased calsequestrin expression in dystrophic mouse skeletal muscle. *Eur. J. Biochem.* **2004**, *271* (19), 3943–3952.

(24) Doran, P.; Martin, G.; Dowling, P.; Jockusch, H.; Ohlendieck, K. Proteome analysis of the dystrophin-deficient MDX diaphragm reveals a drastic increase in the heat shock protein α HSP. *Proteomics* **2006**, *6* (16), 4610–4621.

(25) Stedman, H. H.; Sweeney, H. L.; Shrager, J. B.; Maguire, H. C.; Panettieri, R. A.; Petrof, B.; Narusawa, M.; Leferovich, J. M.; Sladky, J. T.; Kelly, A. M. The mdx mouse diaphragm reproduces the degenerative changes of Duchenne muscular dystrophy. *Nature* **1991**, *352* (6335), 536–539.

(26) Carnwath, J. W.; Shotton, D. M. Muscular dystrophy in the mdx mouse: histopathology of the soleus and extensor digitorum longus muscles. *J. Neurol. Sci.* **1987**, *80* (1), 39–54.

(27) Coulton, G. R.; Morgan, J. E.; Partridge, T. A.; Sloper, J. C. The mdx mouse skeletal muscle myopathy: I. A histological, morphometric and biochemical investigation. *Neuropathol. Appl. Neurobiol.* **1988**, *14* (1), 53–70.

(28) Torres, L. F.; Duchon, L. W. The mutant mdx: inherited myopathy in the mouse. Morphological studies of nerves, muscles and end-plates. *Brain* **1987**, *110* (Pt. 2), 269–299.

(29) Mouisel, E.; Vignaud, A.; Hourde, C.; Butler-Browne, G.; Ferry, A. Muscle weakness and atrophy are associated with decreased regenerative capacity and changes in mTOR signaling in skeletal muscles of venerable (18–24-month-old) dystrophic mdx mice. *Muscle Nerve* **2010**, *41* (6), 809–818.

(30) Lewis, C.; Carberry, S.; Ohlendieck, K. Proteomic profiling of x-linked muscular dystrophy. *J. Muscle Res. Cell Motil.* **2009**, *30* (7–8), 267–269.

(31) Ge, Y.; Molloy, M. P.; Chamberlain, J. S.; Andrews, P. C. Differential expression of the skeletal muscle proteome in mdx mice at different ages. *Electrophoresis* **2004**, *25* (15), 2576–2585.

(32) Cooper, B. J.; Winand, N. J.; Stedman, H.; Valentine, B. A.; Hoffman, E. P.; Kunkel, L. M.; Scott, M. O.; Fischbeck, K. H.; Kornegay, J. N.; Avery, R. J.; et al. The homologue of the Duchenne locus is defective in X-linked muscular dystrophy of dogs. *Nature* **1988**, *334* (6178), 154–156.

(33) Valentine, B. A.; Cooper, B. J.; de Lahunta, A.; O'Quinn, R.; Blue, J. T. Canine X-linked muscular dystrophy. An animal model of Duchenne muscular dystrophy: clinical studies. *J. Neurol. Sci.* **1988**, *88* (1–3), 69–81.

(34) Gygi, S. P.; Rochon, Y.; Franza, B. R.; Aebersold, R. Correlation between protein and mRNA abundance in yeast. *Mol. Cell Biol.* **1999**, *19* (3), 1720–1730.

(35) Handschin, C. Peroxisome proliferator-activated receptor-gamma coactivator-1alpha in muscle links metabolism to inflammation. *Clin. Exp. Pharmacol. Physiol.* **2009**, *36* (12), 1139–1143.

(36) Valentine, B. A.; Cooper, B. J.; Cummings, J. F.; deLahunta, A. Progressive muscular dystrophy in a golden retriever dog: light microscope and ultrastructural features at 4 and 8 months. *Acta Neuropathol.* **1986**, *71* (3–4), 301–310.

(37) Lillie, R., *Histopathologic Technic and Practical Histochemistry*, 3rd ed.; McGraw-Hill: New York, 1965.

(38) Puente, L. G.; Voisin, S.; Lee, R. E.; Megoney, L. A. Reconstructing the regulatory kinase pathways of myogenesis from phosphopeptide data. *Mol. Cell Proteomics* **2006**, *5* (12), 2244–2251.

(39) Ranish, J. A.; Brand, M.; Aebersold, R. *Quantitative Proteomics by Mass Spectrometry. Methods Mol Biol.* **2007**, *359*, 17–35.

(40) Eng, J.; McCormack, A. L.; Yates, J. R. An approach to correlate tandem mass spectral data of peptides with amino acid sequences in protein databases. *J. Am. Soc. Mass Spectrom.* **1994**, *5*, 976–989.

(41) Keller, A.; Nesvizhskii, A. I.; Kolker, E.; Aebersold, R. Empirical statistical model to estimate the accuracy of peptide identifications made by MS/MS and database search. *Anal. Chem.* **2002**, *74* (20), 5383–5392.

- (42) Nesvizhskii, A. I.; Aebersold, R. Analysis, statistical validation and dissemination of large-scale proteomics datasets generated by tandem MS. *Drug Discovery Today* **2004**, *9* (4), 173–181.
- (43) von Haller, P. D.; Yi, E.; Donohoe, S.; Vaughn, K.; Keller, A.; Nesvizhskii, A. I.; Eng, J.; Li, X. J.; Goodlett, D. R.; Aebersold, R.; Watts, J. D. The application of new software tools to quantitative protein profiling via isotope-coded affinity tag (ICAT) and tandem mass spectrometry: II. Evaluation of tandem mass spectrometry methodologies for large-scale protein analysis, and the application of statistical tools for data analysis and interpretation. *Mol. Cell. Proteomics* **2003**, *2* (7), 428–442.
- (44) Li, X. J.; Zhang, H.; Ranish, J. A.; Aebersold, R. Automated statistical analysis of protein abundance ratios from data generated by stable-isotope dilution and tandem mass spectrometry. *Anal. Chem.* **2003**, *75* (23), 6648–6657.
- (45) Matsumura, K.; Tome, F. M.; Collin, H.; Leturcq, F.; Jeanpierre, M.; Kaplan, J. C.; Fardeau, M.; Campbell, K. P. Expression of dystrophin-associated proteins in dystrophin-positive muscle fibers (revertants) in Duchenne muscular dystrophy. *Neuromuscular Disord.* **1994**, *4* (2), 115–120.
- (46) Yuan, J. S.; Reed, A.; Chen, F.; Stewart, C. N., Jr. Statistical analysis of real-time PCR data. *BMC Bioinf.* **2006**, *7*, 85.
- (47) Ashburner, M.; Ball, C. A.; Blake, J. A.; Botstein, D.; Butler, H.; Cherry, J. M.; Davis, A. P.; Dolinski, K.; Dwight, S. S.; Eppig, J. T.; Harris, M. A.; Hill, D. P.; Issel-Tarver, L.; Kasarskis, A.; Lewis, S.; Matese, J. C.; Richardson, J. E.; Ringwald, M.; Rubin, G. M.; Sherlock, G. Gene ontology: tool for the unification of biology. The Gene Ontology Consortium. *Nat. Genet.* **2000**, *25* (1), 25–29.
- (48) Maglott, D.; Ostell, J.; Pruitt, K. D.; Tatusova, T. Entrez Gene: gene-centered information at NCBI. *Nucleic Acids Res.* **2007**, *35* (Database issue), D26–31.
- (49) Sayers, E. W.; Barrett, T.; Benson, D. A.; Bryant, S. H.; Canese, K.; Chetverin, V.; Church, D. M.; DiCuccio, M.; Edgar, R.; Federhen, S.; Feolo, M.; Geer, L. Y.; Helmberg, W.; Kapustin, Y.; Landsman, D.; Lipman, D. J.; Madden, T. L.; Maglott, D. R.; Miller, V.; Mizrahi, I.; Ostell, J.; Pruitt, K. D.; Schuler, G. D.; Sequeira, E.; Sherry, S. T.; Shumway, M.; Sirotkin, K.; Souvorov, A.; Starchenko, G.; Tatusova, T. A.; Wagner, L.; Yaschenko, E.; Ye, J. Database resources of the National Center for Biotechnology Information. *Nucleic Acids Res.* **2009**, *37* (Database issue), D5–15.
- (50) Puente, L. G.; Borris, D. J.; Carriere, J. F.; Kelly, J. F.; Megeney, L. A. Identification of candidate regulators of embryonic stem cell differentiation by comparative phosphoprotein affinity profiling. *Mol Cell Proteomics* **2006**, *5* (1), 57–67.
- (51) Han, X.; Gross, R. W. Quantitative analysis and molecular species fingerprinting of triacylglyceride molecular species directly from lipid extracts of biological samples by electrospray ionization tandem mass spectrometry. *Anal. Biochem.* **2001**, *295* (1), 88–100.
- (52) Hojlund, K.; Yi, Z.; Hwang, H.; Bowen, B.; Lefort, N.; Flynn, C. R.; Langlais, P.; Weintraub, S. T.; Mandarin, L. J. Characterization of the human skeletal muscle proteome by one-dimensional gel electrophoresis and HPLC-ESI-MS/MS. *Mol. Cell. Proteomics* **2008**, *7* (2), 257–267.
- (53) Kim, R. H.; Peters, M.; Jang, Y.; Shi, W.; Pintlilie, M.; Fletcher, G. C.; DeLuca, C.; Liepa, J.; Zhou, L.; Snow, B.; Binari, R. C.; Manoukian, A. S.; Bray, M. R.; Liu, F. F.; Tsao, M. S.; Mak, T. W. DJ-1, a novel regulator of the tumor suppressor PTEN. *Cancer Cell* **2005**, *7* (3), 263–273.
- (54) Villa-Moruzzi, E.; Puntoni, F.; Marin, O. Activation of protein phosphatase-1 isoforms and glycogen synthase kinase-3 beta in muscle from mdx mice. *Int. J. Biochem. Cell Biol.* **1996**, *28* (1), 13–22.
- (55) Mootha, V. K.; Lindgren, C. M.; Eriksson, K. F.; Subramanian, A.; Sihag, S.; Lehar, J.; Puigserver, P.; Carlsson, E.; Ridderstrale, M.; Laurila, E.; Houstis, N.; Daly, M. J.; Patterson, N.; Mesirov, J. P.; Golub, T. R.; Tamayo, P.; Spiegelman, B.; Lander, E. S.; Hirschhorn, J. N.; Altshuler, D.; Groop, L. C. PGC-1alpha-responsive genes involved in oxidative phosphorylation are coordinately downregulated in human diabetes. *Nat. Genet.* **2003**, *34* (3), 267–273.
- (56) Subramanian, A.; Tamayo, P.; Mootha, V. K.; Mukherjee, S.; Ebert, B. L.; Gillette, M. A.; Paulovich, A.; Pomeroy, S. L.; Golub, T. R.; Lander, E. S.; Mesirov, J. P. Gene set enrichment analysis: a knowledge-based approach for interpreting genome-wide expression profiles. *Proc. Natl. Acad. Sci. U.S.A.* **2005**, *102* (43), 15545–15550.
- (57) Arany, Z. PGC-1 coactivators and skeletal muscle adaptations in health and disease. *Curr. Opin. Genet. Dev.* **2008**, *18* (5), 426–434.
- (58) Arnold, A. S. [PGC-1alpha controls neuromuscular junction and offers a novel therapeutic target in Duchenne dystrophy?]. *Med. Sci. (Paris)* **2007**, *23* (11), 1034–1036.
- (59) Haslett, J. N.; Sanoudou, D.; Kho, A. T.; Bennett, R. R.; Greenberg, S. A.; Kohane, I. S.; Beggs, A. H.; Kunkel, L. M. Gene expression comparison of biopsies from Duchenne muscular dystrophy (DMD) and normal skeletal muscle. *Proc. Natl. Acad. Sci. U.S.A.* **2002**, *99* (23), 15000–15005.
- (60) Pescatori, M.; Broccolini, A.; Minetti, C.; Bertini, E.; Bruno, C.; D'Amico, A.; Bernardini, C.; Mirabella, M.; Silvestri, G.; Giglio, V.; Modoni, A.; Pedemonte, M.; Tasca, G.; Galluzzi, G.; Mercuri, E.; Tonali, P. A.; Ricci, E. Gene expression profiling in the early phases of DMD: a constant molecular signature characterizes DMD muscle from early postnatal life throughout disease progression. *FASEB J.* **2007**, *21* (4), 1210–1226.
- (61) Griffin, J. L.; Des Rosiers, C. Applications of metabolomics and proteomics to the mdx mouse model of Duchenne muscular dystrophy: lessons from downstream of the transcriptome. *Genome Med.* **2009**, *1* (3), 32.
- (62) Ge, Y.; Molloy, M. P.; Chamberlain, J. S.; Andrews, P. C. Proteomic analysis of mdx skeletal muscle: Great reduction of adenylate kinase 1 expression and enzymatic activity. *Proteomics* **2003**, *3* (10), 1895–1903.
- (63) Chen, Y. W.; Zhao, P.; Borup, R.; Hoffman, E. P. Expression profiling in the muscular dystrophies: identification of novel aspects of molecular pathophysiology. *J. Cell Biol.* **2000**, *151* (6), 1321–1336.
- (64) Kuznetsov, A. V.; Winkler, K.; Wiedemann, F. R.; von Bossanyi, P.; Dietzmann, K.; Kunz, W. S. Impaired mitochondrial oxidative phosphorylation in skeletal muscle of the dystrophin-deficient mdx mouse. *Mol. Cell. Biochem.* **1998**, *183* (1–2), 87–96.
- (65) Millay, D. P.; Sargent, M. A.; Osinska, H.; Baines, C. P.; Barton, E. R.; Vuagniaux, G.; Sweeney, H. L.; Robbins, J.; Molkentin, J. D. Genetic and pharmacologic inhibition of mitochondrial-dependent necrosis attenuates muscular dystrophy. *Nat. Med.* **2008**, *14* (4), 442–447.
- (66) Wu, Z.; Puigserver, P.; Andersson, U.; Zhang, C.; Adelman, G.; Mootha, V.; Troy, A.; Cinti, S.; Lowell, B.; Scarpulla, R. C.; Spiegelman, B. M. Mechanisms controlling mitochondrial biogenesis and respiration through the thermogenic coactivator PGC-1. *Cell* **1999**, *98* (1), 115–124.
- (67) Lin, J.; Wu, H.; Tarr, P. T.; Zhang, C. Y.; Wu, Z.; Boss, O.; Michael, L. F.; Puigserver, P.; Isotani, E.; Olson, E. N.; Lowell, B. B.; Bassel-Duby, R.; Spiegelman, B. M. Transcriptional co-activator PGC-1 alpha drives the formation of slow-twitch muscle fibres. *Nature* **2002**, *418* (6899), 797–801.
- (68) Wenz, T.; Diaz, F.; Spiegelman, B. M.; Moraes, C. T. Activation of the PPAR/PGC-1alpha pathway prevents a bioenergetic deficit and effectively improves a mitochondrial myopathy phenotype. *Cell Metab.* **2008**, *8* (3), 249–256.
- (69) Handschin, C.; Kobayashi, Y. M.; Chin, S.; Seale, P.; Campbell, K. P.; Spiegelman, B. M. PGC-1alpha regulates the neuromuscular junction program and ameliorates Duchenne muscular dystrophy. *Genes Dev.* **2007**, *21* (7), 770–783.
- (70) Miura, P.; Chakkalakal, J. V.; Boudreault, L.; Belanger, G.; Hebert, R. L.; Renaud, J. M.; Jasmin, B. J. Pharmacological activation of PPAR{beta}/{delta} stimulates utrophin A expression in skeletal muscle fibers and restores sarcolemmal integrity in mature mdx mice. *Hum. Mol. Genet.* **2009**, *18*, 4640–4649.
- (71) Lennon, N. J.; Kho, A.; Bacskai, B. J.; Perlmutter, S. L.; Hyman, B. T.; Brown, R. H., Jr. Dysferlin interacts with annexins A1 and A2 and mediates sarcolemmal wound-healing. *J. Biol. Chem.* **2003**, *278* (50), 50466–50473.

(72) Hubbard, M. J.; Cohen, P. On target with a new mechanism for the regulation of protein phosphorylation. *Trends Biochem. Sci.* **1993**, *18* (5), 172–177.

(73) Dent, P.; MacDougall, L. K.; MacKintosh, C.; Campbell, D. G.; Cohen, P. A myofibrillar protein phosphatase from rabbit skeletal muscle contains the beta isoform of protein phosphatase-1 complexed to a regulatory subunit which greatly enhances the dephosphorylation of myosin. *Eur. J. Biochem.* **1992**, *210* (3), 1037–1044.

(74) Dogra, C.; Changotra, H.; Wergedal, J. E.; Kumar, A. Regulation of phosphatidylinositol 3-kinase (PI3K)/Akt and nuclear factor-kappa B signaling pathways in dystrophin-deficient skeletal muscle in response to mechanical stretch. *J. Cell Physiol.* **2006**, *208* (3), 575–585.

(75) Lang, J. M.; Esser, K. A.; Dupont-Versteegden, E. E. Altered activity of signaling pathways in diaphragm and tibialis anterior muscle of dystrophic mice. *Exp. Biol. Med. (Maywood, NJ, U.S.)* **2004**, *229* (6), 503–511.

(76) Blaauw, B.; Canato, M.; Agatea, L.; Toniolo, L.; Mammucari, C.; Masiero, E.; Abraham, R.; Sandri, M.; Schiaffino, S.; Reggiani, C. Inducible activation of Akt increases skeletal muscle mass and force without satellite cell activation. *FASEB J.* **2009**, *23*, 3896–3905.

(77) Zhong, N.; Xu, J. Synergistic activation of the human MnSOD promoter by DJ-1 and PGC-1alpha: regulation by SUMOylation and oxidation. *Hum. Mol. Genet.* **2008**, *17* (21), 3357–3367.